

Explicit calculation of the two-loop corrections to the chiral magnetic effect with the NJL model

Kit-fai Chu, Peng-hui Huang, and Hui Liu*

Physics Department and Siyuan Laboratory, Jinan University, Guangzhou 510632, China



(Received 28 February 2018; published 21 May 2018)

The chiral magnetic effect (CME) is usually believed to not receive higher-order corrections due to the nonrenormalization of the AVV triangle diagram in the framework of quantum field theory. However, the CME-relevant triangle, which is obtained by expanding the current-current correlation, requires zero momentum on the axial vertex and is not equivalent to the general AVV triangle when taking the zero-momentum limit owing to the infrared problem on the axial vertex. Therefore, it is still significant to check if there exists perturbative higher-order corrections to the current-current correlation. In this paper, we explicitly calculate the two-loop corrections of CME within the Nambu-Jona-Lasinio model with a Chern-Simons term, which ensures a consistent μ_5 . The result shows the two-loop corrections to the CME conductivity are zero, which confirms the nonrenormalization of CME conductivity.

DOI: [10.1103/PhysRevD.97.096009](https://doi.org/10.1103/PhysRevD.97.096009)

I. INTRODUCTION

The electric current induced by strong magnetic field and chirality imbalance in heavy ion collisions, which is called the chiral magnetic effect (CME) [1–6], has seen rising interest in recent years. It states that in off-central heavy ion collisions a strong magnetic field perpendicular to the collision plane has been generated to induce an electric current due to the nontrivial QCD vacuum configuration [4,7], which is described by

$$n_w = -\frac{N_f g^2}{32\pi^2} \int d^4x \epsilon_{\mu\nu\rho\lambda} F_{\mu\nu}^l F_{\rho\lambda}^l, \quad (1)$$

where a nonzero winding number n_w indicates the imbalance of left-handed and right-handed quarks. Since the spin magnetic moment always tends to be parallel to the external magnetic field by the lowest Landau level, the positive (negative) helicity quark carries current parallel (antiparallel) to its magnetic moment. Hence, the direction of induced current depends on quarks with positive or negative helicity in the majority. As a result, an electric current is induced by the separation of quarks carried opposite electrical charge due to the nonzero axial charge density with P and CP violation. The experiments in the Relativistic Heavy Ion Collider [8–11] and LHC [12] have

reported the some observations of charge separation which might be relevant to CME current.

The CME classical result, i.e., the linear relationship between the induced current and the magnetic field, is often written as

$$\mathbf{J} = \eta \frac{e^2}{2\pi^2} \mu_5 \mathbf{B}, \quad (2)$$

where $\eta = N_c \sum_f q_f^2$, q_f is the charge number of flavor f , and μ_5 is the axial chemical potential. This result can be achieved in various methods, such as balancing the energy, solving the Dirac equation, and from the thermal potential or the effective action [5]. It is also related to the AVV triangle diagram that contains an axial vertex and two vector vertices. The relation of triangle diagram to the CME is also analyzed in the longitudinal and transverse parts of the anomalies [13]. Moreover, the CME can also be studied in the holographic model [14–17], anomalous hydrodynamics [18], and lattice simulation [19,20].

The nonrenormalization of the CME is a rather subtle issue in current publications. In the framework of quantum field theory, the induced electric current can be related to the magnetic field through linear response theory. Therefore, the CME conductivity is proportional to the current-current correlation that contains the parameter μ_5 that describes the imbalance of chirality. Expanding the correlation to the first order of μ_5 is equivalent to transforming the two-point loop diagram to the VVA triangle diagram (see Fig. 1 and also Sec. II), which is protected from higher-order corrections through the well-known Adler-Bardeen theorem [21]. In addition, even introducing the Chern-Simons term into the effective action for a

*tliuhui@jnu.edu.cn

Published by the American Physical Society under the terms of the Creative Commons Attribution 4.0 International license. Further distribution of this work must maintain attribution to the author(s) and the published article's title, journal citation, and DOI. Funded by SCOAP³.

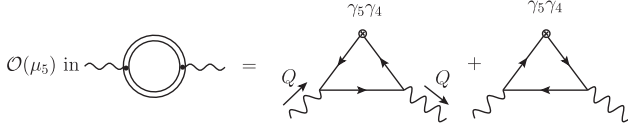


FIG. 1. The sketch of expansion of current-current correlation with respect to the CME. The double line denotes the propagator with μ_5 , while the single line denotes the regular fermion propagator. The cross-vertex denotes the axial vertex with zero-momentum incoming.

consistent μ_5 [22], which guarantees the conservative axial charge, one could also prove that all corrections to the topological mass term vanish identically [23]. Such a nonrenormalization property agrees with the hydrodynamic calculations [18,24] that make people believe the CME receives no higher-order perturbative corrections. However, this is not the whole story. From the lattice point of view, the lattice simulation for the CME disagrees with the classical CME result at the quantitative level [19,20], even though the systematic effects have been considered [25]. Kinetic theory points out that those differences may come from the attractive axial-vector interaction [26]. The interacting lattice model indicates that the CME may receive correction from interfermion interactions that are not relevant in practice [27]. From the quantum field theory point of view, there is an axial vertex with zero momentum on the triangle diagram with respect to the classical CME, which is not equivalent to the general AVV triangle when taking the zero-momentum limit on the axial vertex because of the IR subtlety. As we know, only at the limit order $\lim_{\mathbf{q} \rightarrow 0} \lim_{q_0 \rightarrow 0}$, with (q_0, \mathbf{q}) the 4-momentum of the axial vertex, the general AVV triangle can reproduce the classical CME result [28]. What is more, if introducing the Chern-Simons term, one could prove that the current-current correlation with respect to the CME, which is represented by the AVV triangle with zero incoming momentum at the axial vertex, vanishes at one-loop level [28] so that Eq. (2) is completely contributed by the Chern-Simons term. As far as we know, there is no general argument that suggests the current-current correlation vanishing for all higher-order corrections. The full picture of the higher-order correction of chiral magnetic effect is still ambiguous. In this paper, we aim to calculate the current-current correlation that contributes to the CME current at two-loop level within the NJL model to examine whether the two-loop corrections exist or not.

In Sec. II, we will start from the framework of the chiral magnetic conductivity through the thermal field theory. In Sec. III, we will calculate the two-loop diagrams from the NJL model with Pauli-Villars regularization. Section IV is the conclusion. In this paper, we will adopt the Euclidean metric $\text{diag}(1,1,1,1)$ and the Minkowski 4-momentum $P = (\mathbf{p}, p_0) = (\mathbf{p}, ip_4)$ for p_4 real. All gamma matrices are Hermitian.

II. FRAMEWORK OF CHIRAL MAGNETIC CONDUCTIVITY

Consider the effective Lagrangian density of a massless quark matter with nonzero axial charge,

$$\mathcal{L} = -\frac{1}{4} F_{\mu\nu}^l F_{\mu\nu}^l - \frac{1}{4} F_{\mu\nu} F_{\mu\nu} - \bar{\psi}(\gamma_\mu \partial_\mu - igT^l \gamma_\mu A_\mu^l - ie\hat{q}\gamma_\mu A_\mu)\psi + \mu_5(\bar{\psi}\gamma_4\gamma_5\psi + i\Omega_4), \quad (3)$$

where \hat{q} is the diagonal matrix of electric charge in flavor space and μ_5 is the axial chemical potential. Ω_4 is the fourth component of the Chern-Simons term, which is given by

$$\Omega_\mu = i\frac{N_f g^2}{8\pi^2} \epsilon_{\mu\nu\rho\lambda} A_\nu^l \left(\frac{\partial A_\lambda^l}{\partial x_\rho} - \frac{1}{3} f^{lab} A_\rho^a A_\lambda^b \right) + i\eta \frac{e^2}{4\pi^2} \epsilon_{\mu\nu\rho\lambda} A_\nu \frac{\partial A_\lambda}{\partial x_\rho}, \quad (4)$$

where N_f is the number of the flavor and l is the color index for the $SU(N_c)$ field ($N_c = 3$).

In the thermal field theory, the generating functional of Green's function corresponds to the partition function. Following the general procedure of thermal field theory [28], the electric current can be written as

$$J_i(x) = \frac{\delta\Gamma[\mathcal{A}]}{\delta\mathcal{A}_i(x)} + \eta \frac{e^2}{2\pi^2} \mu_5 \mathcal{B}_i, \quad (5)$$

where \mathcal{A}_i and \mathcal{B}_i are the thermal average of gauge field A_i and magnetic field B_i . The second term of Eq. (5) is generated by the Chern-Simons term. Expanding the action $\Gamma[\mathcal{A}]$ according to \mathcal{A} , one will obtain the current-current correlation as the leading-order coefficient,

$$\Gamma[\mathcal{A}] = \int \frac{d^4 Q}{(2\pi)^4} \left[-\frac{1}{2} \mathcal{A}_\mu^*(Q) \Pi_{\mu\nu}(Q) \mathcal{A}_\nu(Q) + \mathcal{O}(\mathcal{A}^3) \right]. \quad (6)$$

Therefore, the induced current is given by

$$J_i(Q) = \mathcal{K}_{ij} \mathcal{A}_j(Q), \quad (7)$$

where

$$\mathcal{K}_{ij} = -\Pi_{ij}(Q) - i\eta \frac{e^2}{2\pi^2} \mu_5 \epsilon_{ijk} q_k + \mathcal{O}(\mathcal{A}^2). \quad (8)$$

Regarding to the chiral magnetic conductivity, we need to isolate the coefficient of $\mu_5 \epsilon_{ijk} q_k$ in Π_{ij} .

Obviously, the second term of Eq. (8) originates from the Chern-Simons term, which is protected from higher-order corrections, while the first term is a two-point correlation function that may receive decorations from QCD. These

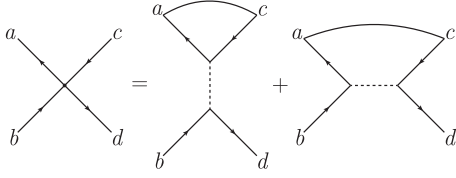


FIG. 2. The four-fermion interaction in which the first diagram on the right-hand side refers to the direct term and the second diagram refers to the exchange term.

decorations run rather complicated at two-loop or higher levels; thus, we introduce the NJL model to simulate the QCD interactions in which the four-fermion interactions instead of the non-Abelian gauge field will greatly reduce the complications in calculation. The interacting part of NJL Lagrangian is given by

$$\mathcal{L}_{\text{int}}^{\text{NJL}} = -GV_{\mu}(x)V_{\mu}(x) = -G(\bar{\psi}\gamma_{\mu}\psi)^2, \quad (9)$$

with G the coupling constant. Notice that a momentum space cutoff Λ is provided in $g^2 = G\Lambda^2$. Notice that the interaction in Eq. (9) contains both direct and exchange terms, which corresponds to two types of contractions that are shown in Fig. 2. By introducing the Fierz transformation, one obtains the Lagrangian

$$\mathcal{L}_{\text{int}}^{\text{NJL}} = G[(\bar{\psi}\psi)^2 - (\bar{\psi}\gamma_5\psi)^2] - \frac{3G}{2}(\bar{\psi}\gamma_{\mu}\psi)^2 - \frac{G}{2}(\bar{\psi}\gamma_{\mu}\gamma_5\psi)^2, \quad (10)$$

where only direct interactions are involved. It is easy to verify that only the last two terms of Eq. (10) have a nonzero contribution owing to the traces of the gamma matrix. Therefore, all we need to compute are the six diagrams in Fig. 3, in which the single- or double-dashed lines correspond to the vector and axial-vector direct coupling, not propagators.

III. TWO-LOOP CORRECTIONS

Following the effective Lagrangian, Eq. (3), one can read out the free quark propagator with a 4-momentum $P = (\mathbf{p}, p_0) = (\mathbf{p}, ip_4)$,

$$S_F(P|m) = \frac{i}{\not{P} + \mu_5\gamma_4\gamma_5 - m}, \quad (11)$$

where m is the quark mass and $\not{P} = \gamma_4 p_4 - i\boldsymbol{\gamma} \cdot \mathbf{p}$. In our calculation, we consider light quarks; i.e., the quark mass will be set to zero. But since we involve Pauli-Villars regularization to guarantee the charge conservation, we keep the mass in the format of the propagator. In the following calculation and statement in Fig. 3, the color-flavor factor η is suppressed, and the main figure number is

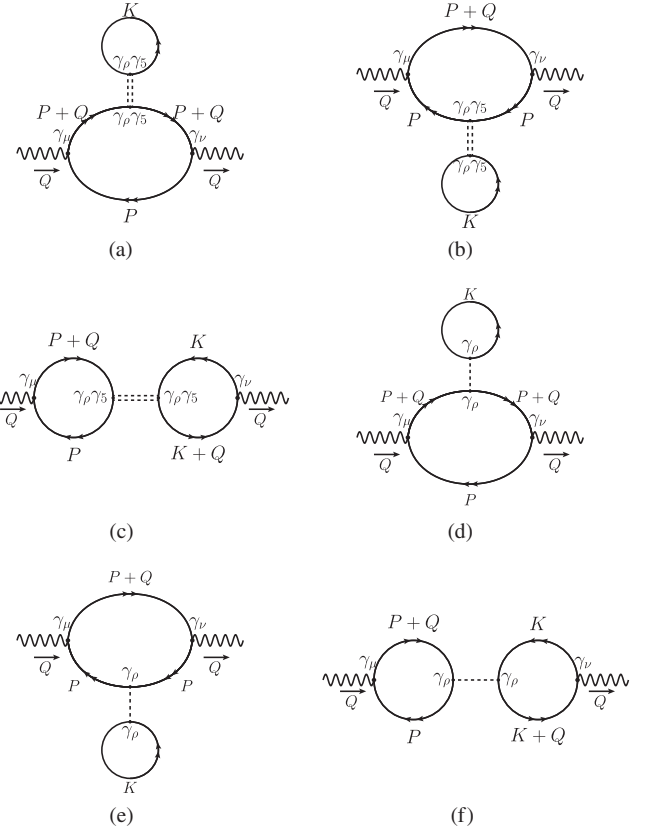


FIG. 3. Feynman diagrams of the two-loop current-current correlation. The solid fermion line represents the propagator with μ_5 . The dashed line and double dashed lines represent the coupling of vector vertex and axial-vector vertex, respectively.

omitted so that part (a) refers to Fig. 3(a) and so on and so forth. To compare to the classical CME conductivity, we focus on the static limit $\omega = 0$ and concern ourselves with the term that contains the structure like $\mu_5 q_k \epsilon_{ijk}$ in Π_{ij} . In the following calculations, the terms that are irrelevant with such structure are neglected.

A. Figures 3(a) and 3(b)

Let us begin with Figs. 3(a) and 3(b). Notice that the small loops with momentum K in these two diagrams are the same; one can extract it out and denote it by Λ_{ρ}^A , where the superscript A means axial-vertex coupling, and explain Figs. 3(a) and 3(b) as

$$\Pi_{\mu\nu}^{a+b} \equiv \Lambda_{\rho}^A \times (\Xi_{\rho\mu\nu}^{A,a} + \Xi_{\rho\mu\nu}^{A,b}), \quad (12)$$

where $\Xi_{\rho\mu\nu}^{A,a}$ and $\Xi_{\rho\mu\nu}^{A,b}$ represent the big loop in Figs. 3(a) and 3(b), respectively. The explicit expressions for Λ_{ρ}^A , $\Xi_{\rho\mu\nu}^{A,a}$, and $\Xi_{\rho\mu\nu}^{A,b}$ are

$$\Lambda_\rho^A = \frac{G}{2} iT \sum_{k_4} \int \frac{d^3 \mathbf{k}}{(2\pi)^3} \text{tr} \left[\frac{i}{\mathcal{K} + \mu_5 \gamma_4 \gamma_5} \gamma_\rho \gamma_5 + \sum_{s'=1} C_{s'} \frac{i}{\mathcal{K} + \mu_5 \gamma_4 \gamma_5 - M_{s'}} \gamma_\rho \gamma_5 \right] \quad (13)$$

and

$$\begin{aligned} \Xi_{\rho\mu\nu}^{A,a}(Q) = ie^2 T \sum_{p_4} \int \frac{d^3 \mathbf{p}}{(2\pi)^3} \text{tr} & \left[\frac{i}{\mathcal{P}l + \mu_5 \gamma_4 \gamma_5} \gamma_\rho \gamma_5 \frac{i}{\mathcal{P}l + \mu_5 \gamma_4 \gamma_5} \gamma_\mu \frac{i}{\mathcal{P} + \mu_5 \gamma_4 \gamma_5} \gamma_\nu \right. \\ & \left. + \sum_{s=1} C_s \frac{i}{\mathcal{P}l + \mu_5 \gamma_4 \gamma_5 - M_s} \gamma_\rho \gamma_5 \frac{i}{\mathcal{P}l + \mu_5 \gamma_4 \gamma_5 - M_s} \gamma_\mu \frac{i}{\mathcal{P} + \mu_5 \gamma_4 \gamma_5 - M_s} \gamma_\nu \right] \end{aligned} \quad (14)$$

$$\begin{aligned} \Xi_{\rho\mu\nu}^{A,b}(Q) = ie^2 T \sum_{p_4} \int \frac{d^3 \mathbf{p}}{(2\pi)^3} \text{tr} & \left[\frac{i}{\mathcal{P}l + \mu_5 \gamma_4 \gamma_5} \gamma_\mu \frac{i}{\mathcal{P} + \mu_5 \gamma_4 \gamma_5} \gamma_\rho \gamma_5 \frac{i}{\mathcal{P} + \mu_5 \gamma_4 \gamma_5} \gamma_\nu \right. \\ & \left. + \sum_{s=1} C_s \frac{i}{\mathcal{P}l + \mu_5 \gamma_4 \gamma_5 - M_s} \gamma_\mu \frac{i}{\mathcal{P} + \mu_5 \gamma_4 \gamma_5 - M_s} \gamma_\rho \gamma_5 \frac{i}{\mathcal{P} + \mu_5 \gamma_4 \gamma_5 - M_s} \gamma_\nu \right], \end{aligned} \quad (15)$$

where $P' = P + Q$. Pauli-Villars regulators are involved, the coefficients of which are restricted by the condition

$$\sum_{s=1} C_s = -1 \quad \text{or} \quad \sum_{s=0} C_s = 0. \quad (16)$$

First, we expand the spatial component of Eq. (13) to the linear order of μ_5 and complete the trace and obtain

$$\begin{aligned} \Lambda_i^A = 4GT\mu_5 \sum_{s'=0} C_{s'} \sum_{k_4} \int \frac{d^3 \mathbf{k}}{(2\pi)^3} \frac{k_4 k_i}{(-k_4^2 - \mathbf{k}^2 - M_{s'}^2)^2} \\ + \mathcal{O}(\mu_5^2), \end{aligned} \quad (17)$$

where we applied a more compact resummation form with $M_0 = 0$ and $C_0 = 1$. Notice that the sum over Matsubara frequencies k_4 is applied on an odd function of k_4 ; we conclude that the linear μ_5 term of Λ_i^A becomes zero.

Then, we consider the temporal component Λ_4^A , which is contracted with $\Xi_{4\mu\nu}$. Since the leading order of Λ_4^A is linear to μ_5 , it is sufficient to consider the zeroth order of μ_5 in $\Xi_{4\mu\nu}$. In the following calculation, we will suppress the index 4 for convenience. The contribution of Fig. 3(a) is given by

$$\begin{aligned} \Xi_{\mu\nu}^{A,a}(Q) = ie^2 \sum_{s=0} C_s \times T \sum_{p_4} \int \frac{d^3 \mathbf{p}}{(2\pi)^3} \\ \times \text{tr} \left[\frac{i}{\mathcal{P}l - M_s} \gamma_\rho \gamma_5 \frac{i}{\mathcal{P}l - M_s} \gamma_\mu \frac{i}{\mathcal{P} - M_s} \gamma_\nu \right]. \end{aligned} \quad (18)$$

The introduction of series of Pauli-Villars regulator cancels out all UV divergences, and there has applied a more compact resummation form with $M_0 = 0$. After straightforward evaluation on the trace, we expand the expression in terms of q and single out its linear terms, which yields

$$\begin{aligned} \Xi_{ij}^{A,a}(0, q) = -4ie^2 \epsilon_{ijk} q_k \sum_{s=0} C_s \times T \sum_{p_4} \int \frac{d^3 \mathbf{p}}{(2\pi)^3} \\ \times \frac{2p_4^2 - \frac{2}{3}p^2 + 2M_s^2}{[-p_4^2 - (p^2 + M_s^2)]^3}, \end{aligned} \quad (19)$$

where $\mu = i$, $\nu = j$, and $\int d^3 \mathbf{p} p_l p_k \rightarrow \int d^3 \mathbf{p} \frac{1}{3} p^2 \delta_{lk}$ are applied.

Following the same steps, we can handle Ξ_{ij}^b , and finally obtain

$$\begin{aligned} \Xi_{ij}^{A,a} + \Xi_{ij}^{A,b} = 4ie^2 \epsilon_{ijk} q_k \sum_{s=0} C_s \times T \sum_{p_4} \int \frac{d^3 \mathbf{p}}{(2\pi)^3} \\ \times \frac{-3p_4^2 + p^2 - 3M_s^2}{[-p_4^2 - (p^2 + M_s^2)]^3}. \end{aligned} \quad (20)$$

After performing the summation on Matsubara frequencies (see Appendix A), we obtain that

$$\begin{aligned} \Xi_{ij}^{A,a} + \Xi_{ij}^{A,b} = 4ie^2 \epsilon_{ijk} q_k \int \frac{d^3 \mathbf{p}}{(2\pi)^3} \left\{ \frac{1}{2p} \frac{\beta^2 e^{\beta p} (e^{\beta p} - 1)}{(e^{\beta p} + 1)^3} \right. \\ \left. + \sum_{s=1} C_s \frac{3M_s^2}{4} \frac{1}{(p^2 + M_s^2)^{5/2}} \right\}. \end{aligned} \quad (21)$$

After performing the 3-momentum integration, we obtain

$$\int d^3 \mathbf{p} \frac{1}{2p} \frac{\beta^2 e^{\beta p} (e^{\beta p} - 1)}{(e^{\beta p} + 1)^3} = \pi \quad (22)$$

$$\int d^3 \mathbf{p} \frac{1}{(p^2 + M_s^2)^{5/2}} = \frac{4\pi}{3M_s^2}. \quad (23)$$

Then, the first terms in Eq. (23) cancel each other by considering Eq. (16), which yields

$$\Xi_{ij}^{A,a} + \Xi_{ij}^{A,b} = 0. \quad (24)$$

Therefore, we end up with

$$\Pi_{ij}^{a+b} = 0. \quad (25)$$

B. Figure 3(c)

Figure 3(c) contains two similar loops, each of which is denoted by Θ^A . We write it as

$$\Pi_{\mu\nu}^c \equiv -\frac{G}{2} \Theta_{\mu\rho}^A \times \Theta_{\rho\nu}^A, \quad (26)$$

where

$$\begin{aligned} \Theta_{\mu\rho}^A &= -eT \sum_{s=0} C_s \sum_{p_4} \int \frac{d^3\mathbf{p}}{(2\pi)^3} \\ &\times \text{tr} \left(\frac{i}{\not{p}_l + \mu_5 \gamma_4 \gamma_5 - M_s} \gamma_\mu \frac{i}{\not{p} + \mu_5 \gamma_4 \gamma_5 - M_s} \gamma_\rho \gamma_5 \right). \end{aligned} \quad (27)$$

Since we are aiming at the spatial components of current-current correlation, we set $\mu = i$ and expand it in terms of μ_5 to the linear order as

$$\begin{aligned} \Theta_{i\rho}^A(0, q) &= -eT \sum_{s=0} C_s \sum_{p_4} \int \frac{d^3\mathbf{p}}{(2\pi)^3} \left\{ \frac{-4p_4 \epsilon_{ipk} q_k}{[-p_4^2 - (p^2 + M_s^2)]^2} \right. \\ &\left. + \frac{4i(\frac{8}{3}p^2 p_4 - 2P^2 p_4 - 2M_s^2 p_4) \delta_{i\rho}}{[-p_4^2 - (p^2 + M_s^2)]^3} \mu_5 \right\} + \mathcal{O}(\mu_5^2). \end{aligned}$$

Now, let us look at the summation of Matsubara frequencies in the zeroth order of μ_5 , which reads

$$T \sum_{p_4} \frac{p_4}{[-p_4^2 - (p^2 + M_s^2)]^2}. \quad (28)$$

This summation yields zero because it is an odd function of p_4 , which leads the linear order of μ_5 of Eq. (28) to be zero.

Notice the two loops of Fig. 3(c) have the same structure; thus, its linear order of μ_5 vanishes, i.e.,

$$\Pi_{ij}^c = -\frac{G}{2} \Theta_{i\rho}^A \times \Theta_{\rho j}^A \sim \mathcal{O}(\mu_5^2). \quad (29)$$

Therefore, we end up with

$$\Pi_{ij}^c = 0. \quad (30)$$

C. Figures 3(d) and 3(e)

Like we did in Sec. III A, we extract the small loops in Figs. 3(d) and 3(e) and denote them by Λ_ρ^V , where V

means the vector vertex coupling, and explain Figs. 3(d) and 3(e) as

$$\Pi_{\mu\nu}^{d+e} \equiv \Lambda_\rho^V \times (\Xi_{\rho\mu\nu}^{V,d} + \Xi_{\rho\mu\nu}^{V,e}), \quad (31)$$

where $\Xi_{\rho\mu\nu}^{V,d}$ and $\Xi_{\rho\mu\nu}^{V,e}$ represent the big loop in Figs. 3(d) and 3(e), respectively. The explicit expression for Λ_ρ^V , $\Xi_{\rho\mu\nu}^{V,d}$, and $\Xi_{\rho\mu\nu}^{V,e}$ are

$$\Lambda_\rho^V = \frac{3G}{2} iT \sum_{s'=0} C_{s'} \sum_{k_4} \int \frac{d^3\mathbf{k}}{(2\pi)^3} \text{tr} \left[\frac{i}{\not{K} + \mu_5 \gamma_4 \gamma_5 - M_{s'}} \gamma_\rho \right] \quad (32)$$

and

$$\begin{aligned} \Xi_{\rho\mu\nu}^{V,d}(Q) &= ie^2 T \sum_{s=0} C_s \sum_{p_4} \int \frac{d^3\mathbf{p}}{(2\pi)^3} \left(\frac{i}{\not{p}_l + \mu_5 \gamma_4 \gamma_5 - M_s} \gamma_\rho \right. \\ &\times \frac{i}{\not{p}_l + \mu_5 \gamma_4 \gamma_5 - M_s} \gamma_\mu \frac{i}{\not{p} + \mu_5 \gamma_4 \gamma_5 - M_s} \gamma_\nu \left. \right) \end{aligned} \quad (33)$$

$$\begin{aligned} \Xi_{\rho\mu\nu}^{V,e}(Q) &= ie^2 T \sum_{s=0} C_s \sum_{p_4} \int \frac{d^3\mathbf{p}}{(2\pi)^3} \text{tr} \left(\frac{i}{\not{p}_l + \mu_5 \gamma_4 \gamma_5 - M_s} \gamma_\mu \right. \\ &\times \frac{i}{\not{p} + \mu_5 \gamma_4 \gamma_5 - M_s} \gamma_\rho \frac{i}{\not{p} + \mu_5 \gamma_4 \gamma_5 - M_s} \gamma_\nu \left. \right). \end{aligned} \quad (34)$$

It is easy to check that the term of linear μ_5 vanishes after the trace, and only the zeroth order of μ_5 survives in Eq. (32). However, even in the zeroth order, the spatial components of Λ_ρ^V are zero due to the integration on an odd function; thus, the only nonzero component is

$$\Lambda_4^V = \frac{3}{2} iGT \sum_{s'=0} C_{s'} \sum_{k_4} \int \frac{d^3\mathbf{k}}{(2\pi)^3} \frac{4k_4}{-k_4^2 - \mathbf{k}^2 - M_{s'}^2} + \mathcal{O}(\mu_5^2). \quad (35)$$

After accomplishing the summation on Matsubara frequencies, one ends up with

$$\Lambda_4^V = -3G \sum_{s'=0} C_{s'} \int \frac{d^3\mathbf{k}}{(2\pi)^3}. \quad (36)$$

Considering the regularization condition, Eq. (16), one can conclude that

$$\Pi_{ij}^{d+e} = 0 \quad (37)$$

even without doing the tedious calculation on the big loop of $\Xi_{\rho\mu\nu}^V$.

D. Figure 3(f)

Figure 3(f) contains two similar loops, each of which is denoted by Θ^V . Then, the diagram is interpreted as

$$\Pi_{\mu\nu}^f \equiv -\frac{3G}{2}\Theta_{\mu\rho}^V \times \Theta_{\rho\nu}^V, \quad (38)$$

where

$$\Theta_{\mu\rho}^V(Q) = -eT \sum_{s=0} C_s \sum_{p_4} \int \frac{d^3\mathbf{p}}{(2\pi)^3} \times \text{tr} \left[\frac{i}{\not{p} + \mu_5 \gamma_4 \gamma_5 - M_s} \gamma_\mu \frac{i}{\not{p} + \mu_5 \gamma_4 \gamma_5 - M_s} \gamma_\rho \right]. \quad (39)$$

Expanding Eq. (39) with respect to μ_5 , one finds

$$\Theta_{i\rho}^V = -eT \sum_{s=0} C_s \sum_{p_4} \int \frac{d^3\mathbf{p}}{(2\pi)^3} \left\{ \frac{4(\frac{2}{3}p^2 - P^2 - M_s^2)\delta_{i\rho}}{[-p_4^2 - (p^2 + M_s^2)]^2} + \frac{4i(-3p_4^2 + p^2 - 3M_s^2)\epsilon_{i\rho k} q_k}{[-p_4^2 - (p^2 + M_s^2)]^3} \mu_5 \right\} + \mathcal{O}(\mu_5^2), \quad (40)$$

where we set $\mu = i$. Notice that the integrand of the second term of Eq. (40) is zero, which has been proven in Eq. (20). Since the linear order of μ_5 vanishes in one of the two loops, the product of two similar loops does not contain the linear μ_5 and thus has zero contribution to the CME conductivity, namely,

$$\Pi_{ij}^f = 0. \quad (41)$$

Combining Eqs. (25), (29), (37), and (41), we find that

$$\Pi_{ij}^{a+b+c+d+e+f}(0, q) = 0, \quad (42)$$

which means the contribution from two-loop corrections of current-current correlation is zero so that the classical CME coefficient is completely determined by the Chern-Simons term.

IV. DISCUSSION

In this paper, we calculated the current-current correlation with respect to the CME at two-loop level within the NJL model to check if there are higher-order corrections to the CME current. Some may argue that the CME coefficient is protected by an anomaly so that it is non-renormalized. This argument may come from the fact when one connects the general VVA triangle diagram, which is protected by the Adler-Bardeen theorem, with the CME current by expanding the current-current correlation in terms of μ_5 . However, we should emphasize that the triangle of the CME is not exactly the general triangle but requires a vanishing momentum on the axial vertex. Since the VVA triangle is not IR safe on the axial vertex, the current-current correlation might have the chance to get

higher-order corrections. Although in Ref. [28] the authors proved that the one-loop current-current correlation vanished by the cancellation of the bare loop with its Pauli-Villars regularization, one may still doubt whether is a general case or just a coincidence. Actually, the answer to this question has been partly addressed in Sec. 4 of Ref. [28]. Since we cannot place confidence in the general relation between the triangle anomaly and current-current correlation, an explicit calculation of higher-order corrections is desired. That is the reason why we do this two-loop calculation of the CME current. Fortunately, our result seems to favor that the CME current is free from higher-order corrections because the two-loop correction is still zero.

The problem of higher-order corrections to the CME current is still far from solved since we only addressed the two-loop level within NJL model. A real QCD calculation is desired, although it is rather complicated. Nevertheless, our calculation, as a toy model of QCD, can give us confidence that one may finally find a way to prove that all higher-order corrections vanish for some reason.

ACKNOWLEDGMENTS

We thank Bo Feng, Hai-cang Ren, and Defu Hou for their helpful discussions and suggestions. This work is supported by the National Natural Science Foundation of China under Grant No. 11405074.

APPENDIX A: THE MATSUBARA SUMMATION

In this Appendix, the sum over the Matsubara energy p_4 or k_4 in Sec. III will be illustrated by an alternative method, and an example is provided.

The summation of Matsubara energy $i\omega_n = (2n+1)\pi iT$ corresponding to the fermion can be replaced by a contour integral along the imaginary plane

$$M = T \sum_{p_0} D(p_0 \rightarrow i\omega_n) = \oint \frac{dz}{2\pi i} D(z) f(z) \quad (A1)$$

with the Fermi distribution function

$$f(z) = \frac{1}{e^{\beta z} + 1}, \quad (A2)$$

where the contour integral takes all poles produced by the Fermi distribution function that are equivalent to the summation. Deforming the contour to enclose singularities of $D(z)$, the summation can be completed by summing up residues of $D(z)f(z)$ over singularities of $D(z)$ that

$$M = \sum_{z_i} \text{Res} D(z_i) f(z_i). \quad (A3)$$

For an example, let us consider an expression including singularities that reads

$$I_{\mu\nu}(P) = \frac{H_{\mu\nu}(p_0)}{p_0^2 - p^2}, \quad (\text{A4})$$

where $H_{\mu\nu}$ is an arbitrary function. The sum over Matsubara energy $i\omega_n = (2n+1)\pi iT$ for the fermion is provided by

$$\begin{aligned} T \sum_{p_0} I_{\mu\nu}(p_0, \mathbf{p}) &= T \sum_{p_0} \frac{H_{\mu\nu}(p_0)}{(p_0 + \mathbf{p})(p_0 - \mathbf{p})} \\ &= \oint_C \frac{dz}{2\pi i} \frac{H_{\mu\nu}(z)}{(z + \mathbf{p})(z - \mathbf{p})} \frac{1}{e^{\beta z} + 1} \\ &= f(-\mathbf{p}) \frac{H_{\mu\nu}(-\mathbf{p})}{-2\mathbf{p}} + f(\mathbf{p}) \frac{H_{\mu\nu}(\mathbf{p})}{2\mathbf{p}}. \end{aligned} \quad (\text{A5})$$

APPENDIX B: PAULI-VILLARS REGULARIZATION

The Pauli-Villars (PV) regularization is to replace the normal propagator by a regularized one by adding subtraction terms that contain large mass, i.e.,

$$S_F(P|0) - S_F(P|M) = \frac{i}{\not{p}} - \sum_{s=1} C_s \frac{i}{\not{p} - M_s}, \quad (\text{B1})$$

with M_s the large mass that is going to be infinity after the integration. The series of PV regularization terms with large masses are introduced to ensure that all UV divergence can be removed so that the coefficients C_s in front of each PV regularization term can be chosen as

$$\sum_{s=1} C_s = 1. \quad (\text{B2})$$

If we define $C_0 = 1$, $M_0 = 0$, the regularized propagator may be rewritten in a more compact form as

$$S_F(P) = \sum_{s=0} C_s \frac{i}{\not{p} - M_s}, \quad (\text{B3})$$

and the coefficient condition is thus

$$\sum_{s=0} C_s = 0. \quad (\text{B4})$$

-
- [1] D. E. Kharzeev, *Prog. Part. Nucl. Phys.* **75**, 133 (2014).
[2] D. E. Kharzeev, *Phys. Lett. B* **633**, 260 (2006).
[3] D. E. Kharzeev and A. Zhitnitsky, *Nucl. Phys.* **A797**, 67 (2007).
[4] D. E. Kharzeev, L. D. McLerran, and H. J. Warringa, *Nucl. Phys.* **A803**, 227253 (2008).
[5] K. Fukushima, D. E. Kharzeev, and H. J. Warringa, *Phys. Rev. D* **78**, 074033 (2008).
[6] D. E. Kharzeev and H. J. Warringa, *Phys. Rev. D* **80**, 034028 (2009).
[7] L. McLerran, E. Mottola, and M. E. Shaposhnikov, *Phys. Rev. D* **43**, 2027 (1991).
[8] B. I. Abelev, M. M. Aggarwal, Z. Ahammed, A. V. Alakhverdyants, B. D. Anderson, D. Arkhipkin, G. S. Averichev, J. Balewski, O. Barannikova, and L. S. Barnby, *Phys. Rev. Lett.* **103**, 251601 (2009).
[9] B. I. Abelev *et al.* (STAR Collaboration), *Phys. Rev. C* **81**, 054908 (2010).
[10] STAR Collaboration, *Phys. Rev. C* **88**, 064911 (2013).
[11] L. Adamczyk, J. K. Adkins, G. Agakishiev, M. M. Aggarwal, Z. Ahammed, I. Alekseev, J. Alford, C. D. Anson, A. Aparin, and D. Arkhipkin, *Phys. Rev. Lett.* **113**, 052302 (2014).
[12] B. Abelev, J. Adam, D. Adamov, A. M. Adare, M. M. Aggarwal, R. G. Aglieri, A. G. Agocs, A. Agostinelli, S. S. Aguilar, and Z. Ahammed, *Phys. Rev. Lett.* **110**, 012301 (2013).
[13] P. V. Buividovich, *Nucl. Phys.* **A925**, 218 (2014).
[14] H. U. Yee, *J. High Energy Phys.* 09 (2009) 085.
[15] A. Rebhan, A. Schmitt, and S. A. Stricker, *J. High Energy Phys.* 10 (2010) 026.
[16] A. Gynther, K. Landsteiner, F. Pena-Benitez, and A. Rebhan, *J. High Energy Phys.* 11 (2011) 110.
[17] A. Gorsky, P. N. Kopnin, and A. V. Zayakin, *Phys. Rev. D* **83**, 014023 (2011).
[18] D. T. Son and P. Surówka, *Phys. Rev. Lett.* **103**, 191601 (2009).
[19] P. V. Buividovich, M. N. Chernodub, E. V. Luschevskaya, and M. I. Polikarpov, *Phys. Rev. D* **80**, 054503 (2009).
[20] A. Yamamoto, *Phys. Rev. Lett.* **107**, 031601 (2011).
[21] S. L. Adler and W. A. Bardeen, *Phys. Rev.* **182**, 1517 (1969).
[22] V. A. Rubakov, *arXiv:1005.1888*.
[23] S. Coleman and B. Hill, *Phys. Lett. B* **159**, 184 (1985).
[24] M. V. Isachenkov and A. V. Sadofyev, *Phys. Lett. B* **697**, 404 (2011).
[25] A. Yamamoto, *Phys. Rev. D* **84**, 114504 (2011).
[26] Z. Zhang, *Phys. Rev. D* **85**, 114028 (2012).
[27] P. V. Buividovich, M. Pühr, and S. N. Valgushev, *Phys. Rev. B* **92**, 205122 (2015).
[28] D. F. Hou, H. Liu, and H. C. Ren, *J. High Energy Phys.* 11 (2011) 046.